Title

Sources and transformations of riverine nitrogen across a coastal-plain river network of eastern China: New insights from multiple stable isotopes

Authors

Chen, Wenli

Zhang, Xiaohan

Wu, Nianting

et al.

Publication Date

2024-05-01

DOI

10.1016/j.scitotenv.2024.171671

Peer reviewed

Science of the Total Environment 924 (2024) 171671

Contents lists available at ScienceDirect

Science of the Total Environment

journal homepage: www.elsevier.com/locate/scitotenv

Sources and transformations of riverine nitrogen across a coastal-plain river network of eastern China: New insights from multiple stable isotopes

Wenli Chen [a], Xiaohan Zhang [b], Nianting Wu [b], Can Yuan [b], Yinli Liu [a], Yue Yang [b,c], Zheng Chen [a], Randy A. Dahlgren [d], Minghua Zhang [a,c,d], Xiaoliang Ji [a,*]

[a] Key Laboratory of Watershed Science and Health of Zhejiang Province, School of Public Health and Management, Wenzhou Medical University, Wenzhou 325035, China
[b] Zhejiang Provincial Key Laboratory for Water Environment and Marine Biological Resources Protection, College of Life and Environmental Science, Wenzhou University, Wenzhou 325035, China
[c] Southern Zhejiang Water Research Institute, Wenzhou 325035, China
[d] Department of Land, Air and Water Resources, University of California, Davis, California 95616, USA

HIGHLIGHTS

- NH_4^+-N, NO_3^--N and PN constituted ~45 %, ~30 % and ~20 % of TN in WRT River, respectively.
- Relying only on $\delta^{15}N/\delta^{18}O\text{-}NO_3^-$ failed to present a holistic perspective of N pollution.
- A multi-isotope method was developed to elucidate riverine N sources and fates.
- Nitrification rather than assimilation and denitrification was primary N-cycling process.
- MS was identified as the major TN source (contribution rate was ~50 %) in the WRT River.

GRAPHICAL ABSTRACT

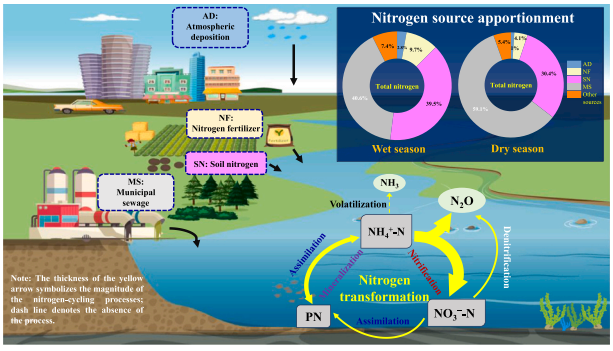

ARTICLE INFO

Editor: Jay Gan

Keywords:
Coastal-plain rivers
Multiple stable isotopes
Nitrogen pollution
Nitrogen biogeochemistry
SIAR model

ABSTRACT

Riverine nitrogen pollution is ubiquitous and attracts considerable global attention. Nitrate is commonly the dominant total nitrogen (TN) constituent in surface and ground waters; thus, stable isotopes of nitrate ($\delta^{15}N/\delta^{18}O\text{-}NO_3^-$) are widely used to differentiate nitrate sources. However, $\delta^{15}N/\delta^{18}O\text{-}NO_3^-$ approach fails to present a holistic perspective of nitrogen pollution for many coastal-plain river networks because diverse nitrogen species contribute to high TN loads. In this study, multiple isotopes, namely, $\delta^{15}N/\delta^{18}O\text{-}NO_3^-$, $\delta^{18}O\text{-}H_2O$, $\delta^{15}N\text{-}NH_4^+$, $\delta^{15}N\text{-}PN$, and $\delta^{15}N^{bulk}/\delta^{18}O/SP\text{-}N_2O$ in the Wen-Rui Tang River, a typical coastal-plain river network of Eastern China, were investigated to identify transformation processes and sources of nitrogen. Then, a stable isotope analysis in R (SIAR) model-TN source apportionment method was developed to quantify the contributions of different nitrogen sources to riverine TN loads. Results showed that nitrogen pollution in the river network was serious with TN concentrations ranging from 1.71 to 8.09 mg/L (mean ± SD: 3.77 ± 1.39 mg/L). Ammonium, nitrate, and suspended particulate nitrogen were the most prominent nitrogen components during the study

* Corresponding author at: Key Laboratory of Watershed Science and Health of Zhejiang Province, Wenzhou Medical University, Wenzhou 325035, Zhejiang Province, China.
E-mail address: jixiao556677@wmu.edu.cn (X. Ji).

https://doi.org/10.1016/j.scitotenv.2024.171671
Received 4 December 2023; Received in revised form 10 March 2024; Accepted 10 March 2024
Available online 11 March 2024

period, constituting 45.4 %, 28.9 %, and 19.9 % of TN, respectively. Multiple hydrochemical and isotopic analysis identified nitrification as the dominant N cycling process. Biological assimilation and denitrification were minor N cycling processes, whereas ammonia volatilization was deemed negligible. Isotopic evidence and SIAR modeling revealed municipal sewage was the dominant contributor to nitrogen pollution. Based on quantitative estimates from the SIAR model, nitrogen source contributions to the Wen-Rui Tang River watershed followed: municipal sewage (40.6 %) ≈ soil nitrogen (39.5 %) > nitrogen fertilizer (9.7 %) > atmospheric deposition (2.8 %) during wet season; and municipal sewage (59.1 %) > soil nitrogen (30.4 %) > nitrogen fertilizer (4.1 %) > atmospheric deposition (1.0 %) during dry season. This study provides a deeper understanding of nitrogen dynamics in eutrophic coastal-plain river networks, which informs strategies for efficient control and remediation of riverine nitrogen pollution.

1. Introduction

Rivers play an important role in maintaining the stability of ecosystem functions and promoting the sustainable development of aquatic environments (Guo et al., 2020; Xuan et al., 2020b; Cao et al., 2022). However, excess nitrogen loads in aquatic ecosystems can induce critical environmental issues (e.g., eutrophication, harmful algae blooms, and hypoxia) and health risks (e.g., "blue baby" syndrome, esophagus/stomach cancer, miscarriage, and birth defects) (Liu et al., 2021; Ye et al., 2021; Guo et al., 2023). Riverine nitrogen concentrations and forms are regulated by the interplay between external pollution sources (e.g., domestic sewage, nitrogen fertilizer, atmospheric deposition, and soil nitrogen) and multiple interacting in-stream biogeochemical transformations (e.g., nitrification, denitrification, ammonia volatilization, and assimilation) (Yi et al., 2017; Liu et al., 2018; Kim et al., 2023).

Eastern China has many coastal-plain river systems whose watersheds are characterized by high population density and intensive anthropogenic activities (Ji et al., 2017). Additionally, these river networks often have stagnant-to-low streamflow and poor connectivity due to the plain topography (i.e., low river gradient), leading to high water residence times and low pollutant export. Given these features, nitrogen pollution in many coastal-plain rivers of Eastern China is a serious ecological threat. In fact, eutrophication and hypoxia (i.e., coastal dead zones) induced by high nitrogen inputs to coastal areas are worldwide environmental issues (Chen et al., 2023a). To design effective nitrogen pollution remediation measures, it is of particular importance to understand the sources and transformations of riverine nitrogen in these watersheds (Dong et al., 2022; Ji et al., 2022a).

Stable isotopes are employed extensively to assist in the identification of nitrogen pollution sources in water bodies (Kohl et al., 1971; Dong et al., 2022). This approach is based on the realization that different nitrogen pollution sources exhibit unique isotopic signatures (Kendall and McDonnell, 1998; Xue et al., 2009). Nitrate (NO_3^--N) is commonly the dominant nitrogen form in the surface and ground waters of agricultural areas; as such, contemporary research primarily focuses on using the dual isotopes $\delta^{15}N/\delta^{18}O$ of NO_3^- to trace NO_3^--N sources and cycling processes (Soto et al., 2019; Torres-Martínez et al., 2020; Zhang et al., 2020; Fackrell et al., 2022). Diverse nitrogen species including ammonium (NH_4^+-N), NO_3^--N, and suspended particulate nitrogen (PN) coexist in coastal-plain river systems owing to the discharge and transformation of nitrogen from multiple nitrogen sources and subsequent in-stream cycling processes. Commonly, total nitrogen (TN) dynamics in plain river networks are dominated by NH_4^+-N and NO_3^--N, and PN also an important nitrogen component (Lian et al., 2020; Xuan et al., 2020a; Lu et al., 2021). Consequently, the $\delta^{15}N/\delta^{18}O$-$NO_3^-$ approach leads to high uncertainty for plain river systems due to the diversity of riverine nitrogen species (Ryu et al., 2021; Zhang et al., 2022). Recent studies demonstrate that the stable isotopic composition of $\delta^{15}N$ in ammonium ($\delta^{15}N$-NH_4^+), suspended particulate nitrogen ($\delta^{15}N$-PN), and the $\delta^{15}N^{bulk}/\delta^{18}O$ and nitrogen site preference (SP) of nitrous oxide ($\delta^{15}N^{bulk}/\delta^{18}O$/SP-$N_2O$) would provide additional information to constrain the identification of nitrogen transformation dynamics and sources (Xuan et al., 2020a; Li et al., 2021; Ye et al., 2021; Zhang et al., 2022). However, few multi-isotope investigations of nitrogen sources and transformations in coastal-plain river systems of Eastern China have been attempted. Until now, little is known about the contributions of potential nitrogen sources to TN pollution for plain river network systems.

This paper hypothesizes that a systematic application of $\delta^{15}N/\delta^{18}O$-$NO_3^-$ along with $\delta^{15}N$-NH_4^+, $\delta^{15}N$-PN, and $\delta^{15}N^{bulk}/\delta^{18}O$/SP-$N_2O$ would greatly enhance our understanding of nitrogen sources and transformations considering $\delta^{15}N/\delta^{18}O$-$NO_3^-$ approach fails to provide a holistic perspective on nitrogen pollution dynamics in plain river systems. Herein, a typical coastal-plain river network located in Eastern China was selected for a multi-isotope investigation. Various hydrochemical parameters and multiple stable isotopes ($\delta^{15}N/\delta^{18}O$-$NO_3^-$, $\delta^{15}N$-NH_4^+, $\delta^{15}N$-PN, $\delta^{18}O$-H_2O, and $\delta^{15}N^{bulk}/\delta^{18}O$/SP-$N_2O$) were analyzed during the wet and dry seasons across multiple watershed sites with contrasting land-use characteristics to: (1) investigate the concentrations and isotopic compositions of different nitrogen species in the river network, (2) elucidate in-stream nitrogen transformation processes at the watershed scale, and (3) identify the primary nitrogen pollution sources and their proportional contributions to the TN loads. This paper expands on the previous studies by Ji et al. (2022a, 2022b) by extending the analysis of stable isotopes from only NO_3^--N to diverse N forms including NO_3^--N, NH_4^+-N, PN, and N_2O. The novelty of this study is the implementation of multiple isotopes and the development of a SIAR model-TN source apportionment method for evaluating riverine TN (not just NO_3^--N) sources and fates across a typical coastal-plain river network of Eastern China for the first time. Results of this study provide quantitative information on nitrogen pollution sources that inform the development and implementation of nitrogen pollution remediation strategies for coastal-plain river networks.

2. Materials and methods

2.1. Study area

The Wen-Rui Tang River watershed is located on the coastal-plain of Eastern China (27°51′–28°02′N latitude, 120°28′–120°46′E longitude; Fig. 1). The watershed covers an area of ~740 km^2 including the central zone of Wenzhou city having a population > 9 million. Total length of the river network is ~1200 km, and the length of the main channel is ~34 km. The watershed experiences a subtropical oceanic climate with an average annual temperature of ~18 °C and a mean annual precipitation of ~1800 mm. Precipitation from April to September accounts for ~70 % of the total rainfall. Considerable anthropogenic pressures affect water quality since the population density exceeds 2000 people/km^2. The urban waterways are mostly hardened, resulting in a small buffer zone for nitrogen retention. The watershed has a diverse land use with forest, residential, and agricultural lands accounting for ~40 %, ~40 %, and ~ 20 % of the study area, respectively (Fig. 1). As a typical coastal-plain river, flows in the Wen-Rui Tang River are relatively quiescent for much of the year, except for periods when the flood-control gates to the adjacent Ou River are open to release flood waters during storm events, such as typhoons.

2.2. Data collection

2.2.1. Sampling

For an effective watershed-scale study in the Wen-Rui Tang River, spatially distributed sampling sites (15 sites) were selected along the mainstream (7 sites) from upstream to downstream and its major tributaries (8 sites) to include the major land-use types as the river flows through farmland, residential, industrial, and wetland areas. Sampling sites 1, 2, 3, 7, 8, 9, and 12 were on the mainstream, and the other sites were located on tributaries: urban sites (3, 5, 9, 10, 11, 12 and 13); suburban sites (1, 2, 6, 7 and 8); industrial sites (4 and 14), and a wetland site (15) (**Fig. S1**). These sampling sites were regarded as representative of nitrogen pollution characteristics of the entire study watershed. Water depths at the sampling sites ranged from 0.7 to 3.8 m (average ~ 2.3 m). To examine seasonal variability of multi-isotope compositions and hydrochemical parameter concentrations, river water sampling campaigns were conducted in June 2022 (wet season) and March 2023 (dry season). In the field, temperature (T), pH, turbidity (TURB), dissolved oxygen (DO), electrical conductivity (EC), and chlorophyll-a (Chl-a) were measured in situ using a multi-parameter probe (YSI EXO2, Xylem, USA). Water samples were collected using a glass hydrophore sampler and immediately placed in 500 mL polyethylene bottles. Additional surface water samples were collected in 250 mL polyethylene bottles preserved with 0.1 mL of saturated $ZnCl_2$ for N_2O analysis at sites 1 (suburban area), 11 (urban area), and 15 (wetland zone) in June 2022 and at all sampling sites in March 2023. All collected water samples were placed in a cooler with dry ice and transported to the laboratory.

Our previous study investigated the site-specific isotopic signatures of atmospheric deposition nitrate, nitrogen fertilizer, and soil nitrogen (Ji et al., 2022a). Herein, to supplement the isotopic composition database for potential nitrogen sources, 10 municipal sewage samples were collected from a local wastewater treatment plant, and 26 atmospheric deposition samples for δ^{15}N-NH_4^+ analysis were collected from six sampling sites during the wet and dry seasons (see Supplementary martials for detailed information about municipal sewage/atmospheric deposition sample collection).

2.2.2. Laboratory analysis

In the laboratory, a subsample of water was filtered using pre-combusted (450 °C for 4 h) glass fiber membranes (Whatman, GF/F, 47 mm diameter) (Tian et al., 2022). Filtered and unfiltered samples were stored in a − 20 °C refrigerator for analysis within 7 days. Filtered samples were used to determine NO_3^--N, nitrite (NO_2^--N), NH_4^+-N, dissolved N (DN), phosphate (PO_4^{3-}-P), major cations/anions, and stable isotope compositions. The unfiltered water samples were used to determine TN, total phosphorus (TP), and total organic carbon (TOC). Colorimetric analyses for NO_3^--N, NO_2^--N, NH_4^+-N, PO_4^{3-}-P, and TN/DN/TP (after alkaline persulfate digestion) were performed on each sample in duplicate using a continuous flow analyzer (Autoanalyser-3, Seal, Germany). Herein, we calculated PN as: PN = TN – DN (Jin et al., 2019) and dissolved organic nitrogen (DON) as: DN – (NO_3^--N + NO_2^--N + NH_4^+-N). TOC concentrations were determined using a TOC analyzer (TOC-L, Shimadzu, Japan). Chloride (Cl^-), fluoride (F^-), and sulfate (SO_4^{2-}) concentrations were determined by ion chromatography (Compact IC plus 882, Metrohm, Switzerland). Major cations (K^+, Ca^{2+}, Na^+, and Mg^{2+}) were measured by inductively coupled plasma mass spectrometry (Thermo iCAP TQ, USA). The HCO_3^- concentrations were determined by dilute hydrochloric acid–methyl orange/phenolphthalein titration. Detection limits were TN/TP/DN ≈ 0.02 mg/L, NO_3^--N/NO_2^--N/NH_4^+-N/PO_4^{3-}-P ≈ 0.003 mg/L, TOC/DOC ≈ 0.1 mg/L, Cl^-/F^-/SO_4^{2-} ≈ 0.1 mg/L, K^+/Ca^{2+} ≈ 100 ng/L, Na^+/Mg^{2+} ≈ 10 ng/L, and HCO_3^- ≈ 5 mg/L.

Samples were transported to the Environmental Stable Isotope Laboratory in Chinese Academy of Agricultural Sciences (Beijing, China) for isotopic analysis. The δ^{15}N/δ^{18}O-NO_3^- values were determined using the bacterial denitrification method. In brief, NO_3^--N was converted to N_2O, and N_2O was then purified by separation before quantification on an isotope ratio mass spectrometer (Delta V plus, Thermo Fisher Scientific, USA). The δ^{15}N-NH_4^+ values were determined by the hypobromite oxidation–hydroxylamine hydrochloride reduction method. Dissolved NH_4^+-N in the water samples was oxidized to NO_2^--N and NO_2^--N was converted to N_2O, which was subsequently determined by isotope ratio mass spectrometry (Isoprime 100, Elementar, UK). δ^{18}O-H_2O was determined using a high-precision water isotope analyzer (L2140-I, Picarro Santa Clara, USA). For suspended δ^{15}N-PN analysis, water samples were filtered through weighed GF/F membranes. A 1 mol/L HCl

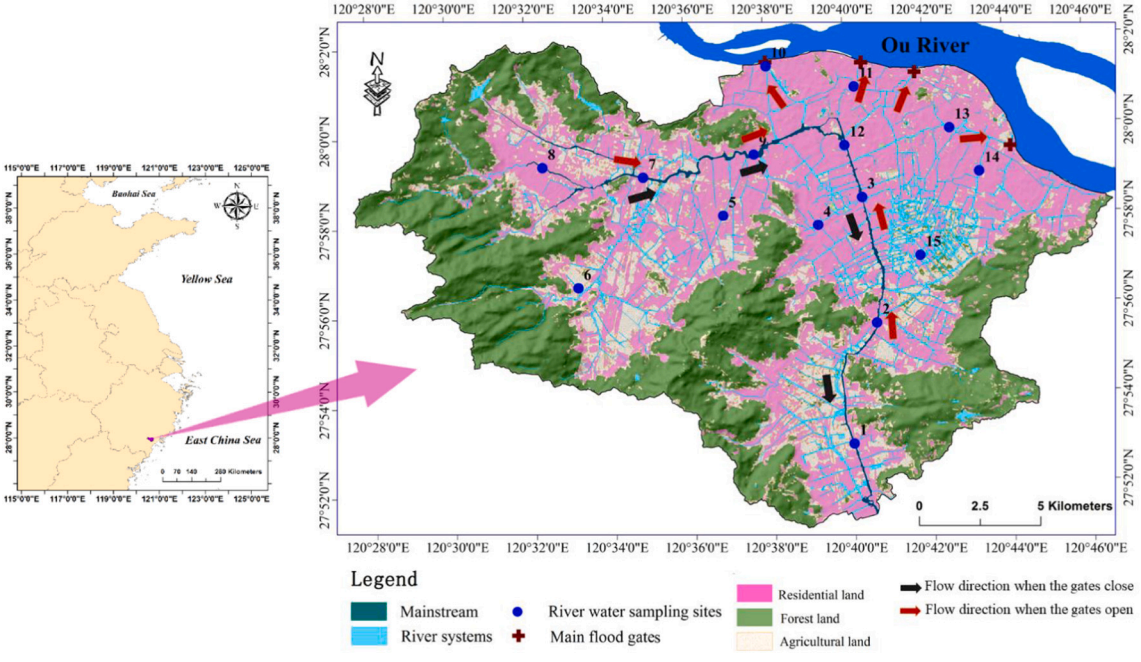

Fig. 1. Location of the Wen-Rui Tang River watershed and sampling sitesalong with dominant land-use classification.

solution was added to the membranes dropwise until completely wetted. Then, the wetted membranes were placed in a desiccator containing concentrated HCl for 48 h. Finally, the membranes were washed repeatedly using ultrapure water until pH ~7 was achieved and subsequently dried for isotopic analysis by isotope ratio mass spectrometry (Isoprime 100, Elementar, UK). The $\delta^{15}N^{bulk}$-N_2O, $\delta^{18}O$-N_2O, and $\delta^{15}N^{\alpha}$-N_2O values were determined with a stable isotope mass spectrometer (Delta V-Precon, Thermo Fisher Scientific, USA). SP-N_2O values were calculated based on $\delta^{15}N^{bulk}$-N_2O and $\delta^{15}N^{\alpha}$-N_2O; additional analytical details can be found in Li et al. (2021). Analytical precisions were as follows: $\delta^{15}N$-NO_3^- (±0.2 ‰), $\delta^{18}O$-NO_3^- (±0.5 ‰), $\delta^{15}N$-NH_4^+ (±0.4 ‰), $\delta^{15}N$-PN (±0.4 ‰), $\delta^{18}O$-H_2O (±0.2 ‰), $\delta^{15}N^{bulk}$-N_2O (±0.5 ‰), $\delta^{15}N^{\alpha}$-N_2O (±0.9 ‰), and $\delta^{18}O$-N_2O (±0.6 ‰).

Stable isotope ratios were expressed in delta (δ) notation as follows:

$$\delta_{sample}(‰) = \left(R_{sample}/R_{standard} - 1\right) \times 1000$$

where R_{sample} and $R_{standard}$ denote sample and standard for $^{15}N/^{14}N$, $^{18}O/^{16}O$ and $^{2}H/^{1}H$, respectively. The $^{15}N/^{14}N$ ratio reference is atmospheric air, while $^{2}H/^{1}H$ and $^{18}O/^{16}O$ references are Vienna Standard Mean Ocean Water.

2.3. Bayesian isotope mixing model

To assess the fractional contributions (%) of different sources to TN, a stable isotope analysis in R (SIAR) model was employed (Parnell et al., 2010). The SIAR model employs the principle of mass balance, with a Dirichlet distribution established as the logical prior distribution. A Markov Chain Monte Carlo random sampling combined with Bayesian updating was utilized to produce posterior distributions of proportional contributions from various sources (Gibrilla et al., 2020). In this study, the SIAR program package was run in R (version 3.1.2). The hybrid model framework can be expressed as follows:

$$X_{ij} = \sum_{k-1}^{k} P_K\left(S_{jk} + C_{jk}\right) + \varepsilon_{ij}$$

$$S_{jk} : N\left(\mu_{jk}, \omega_{jk}^2\right)$$

$$C_{jk} : N\left(\lambda_{jk}, \tau_{jk}^2\right)$$

$$\varepsilon_{jk} : N\left(0, \sigma_j^2\right)$$

where X_{ij} is the isotope value j of the mixture i, in which $I = 1, 2, 3, 4, \ldots$, N and $j = 1, 2, 3, 4, \ldots, J$; S_{jk} denotes the source value k on isotope j (k = 1, 2, 3, 4, …, K) and is normally distributed with a mean of μ_{jk} and standard deviation ω_{jk}; P_k refers to the proportion of source k, as estimated by the SIAR mixing model; C_{jk} represents the isotope fractionation factor for isotope j on source k and is normally distributed with mean λ_{jk} and standard deviation τ_{jk}; and ε_{jk} refers to the unquantified variation between individual mixtures. The analysis employs a normal distribution with a mean of 0 and standard deviation of σ_j. In this study, the model was iterated 500,000 times with a burn-in of 50,000 and a thinning interval of 15. Additional details regarding the SIAR model are documented in Supplementary Materials.

2.4. Total nitrogen source contribution quantification

The mean probability estimate produced by the SIAR model was used to express the contribution from each nitrogen source. The contribution of each source to the TN pollution was determined by calculating the proportion of each nitrogen form to TN and then multiplying it by the corresponding contribution of each source to that nitrogen form. A schematic flowchart of the SIAR model-TN source apportionment method is shown in Fig. 2. Furthermore, we utilized an uncertainty

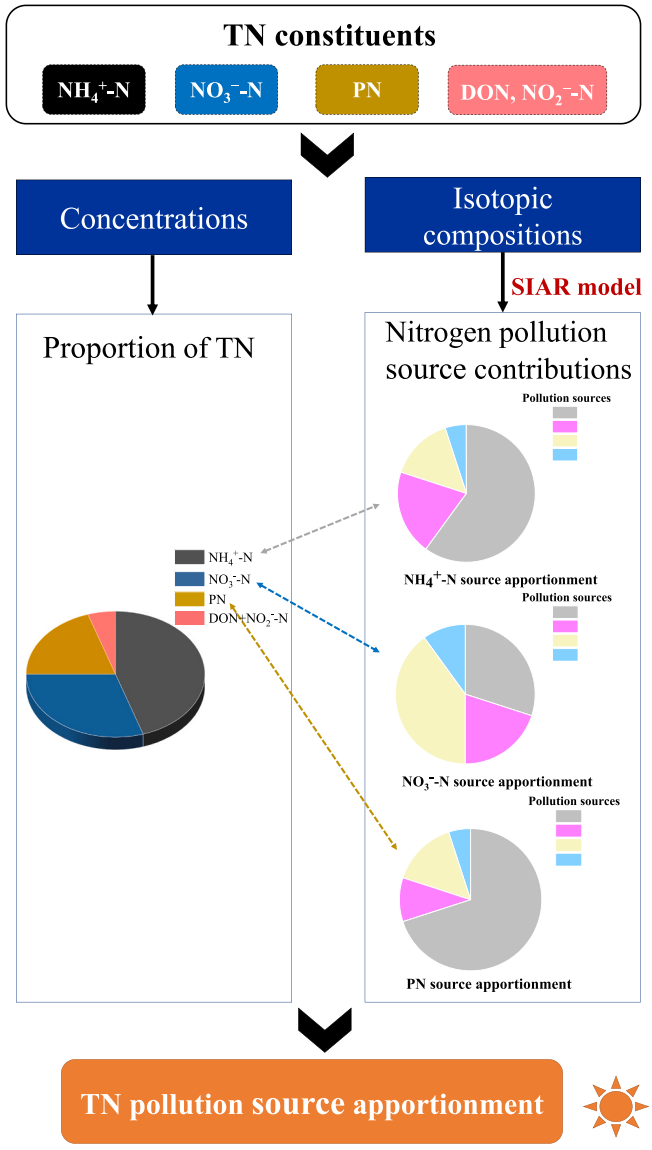

Fig. 2. Schematic flowchart for the nitrogen source apportionment approach utilized in this study.TN: total nitrogen, NO_3^--N: nitrate, NO_2^--N: nitrite, NH_4^+-N: ammonium, DON: dissolved organic nitrogen, PN: particulate nitrogen.

index (UI_{90}), proposed by Ji et al. (2017), to quantify the uncertainty associated with results of the SIAR model-TN source apportionment method. UI_{90} was calculated according to the posterior distributions of different pollution sources produced by SIAR model and defined as the difference between the pollution source contributions at 0.95 cumulative frequency distribution and that at the 0.05 cumulative frequency distribution, and then divided by 0.9. A higher UI_{90} value indicates stronger uncertainty in the apportionment results. Additional details regarding calculation of UI_{90} are described by Shang et al. (2020) and Torres-Martínez et al. (2021a, 2021b).

3. Results and discussion

3.1. Hydrochemical characteristics

Table 1 depicts the summary statistics for the physicochemical parameters of surface waters from the Wen-Rui Tang River in June 2022 (wet season) and March 2023 (dry season). Water temperature exhibited significant spatial and seasonal variations with a higher mean in the wet season (mean ± SD: 30.1 ± 0.7 °C) than in the dry season (16.3 ±

Table 1
Summary of hydrochemical characteristics of the Wen-Rui Tang River network.

Parameters	Whole study period ($N = 30$)			Wet season ($N = 15$)			Dry season (N = 15)		
	Mean ± SD	Minimum	Maximum	Mean ± SD	Minimum	Maximum	Mean ± SD	Minimum	Maximum
T (°C)	23.2 ± 6.9**	15.3	31.7	30.1 ± 0.7	28.6	31.7	16.3 ± 0.8	15.3	17.8
DO (mg/L)	5.8 ± 2.0	3.2	12.3	6.3 ± 2.4	3.5	12.3	5.3 ± 1.3	3.2	8.0
pH	7.51 ± 1.05**	6.15	9.82	8.50 ± 0.48	8.06	9.82	6.53 ± 0.16	6.15	6.80
EC (μS/cm)	262 ± 105	103	532	264 ± 125	103	532	260 ± 79	159	416
TURB (NTU)	20.8 ± 9.9*	6.6	40.0	24.7 ± 11.5	6.6	40.0	16.8 ± 5.6	6.9	25.6
Chl-a (μg/L)	11.4 ± 18.5	0.8	94.3	17.5 ± 24.2	2.3	94.3	5.3 ± 4.5	0.8	18.1
TN (mg/L)	3.77 ± 1.39**	1.71	8.09	2.84 ± 0.78	1.71	4.55	4.71 ± 1.22	3.57	8.09
NH_4^+-N (mg/L)	1.71 ± 1.23*	0.09	5.43	1.19 ± 0.84	0.09	3.30	2.24 ± 1.33	0.78	5.43
NO_3^--N (mg/L)	1.09 ± 0.52	0.27	2.27	0.92 ± 0.45	0.27	1.99	1.26 ± 0.54	0.33	2.27
NO_2^--N (mg/L)	0.10 ± 0.04*	0.04	0.28	0.08 ± 0.03	0.04	0.13	0.12 ± 0.05	0.08	0.28
PN (mg/L)	0.75 ± 0.35*	0.27	1.60	0.52 ± 0.18	0.27	1.00	0.98 ± 0.32	0.47	1.60
TP (mg/L)	0.23 ± 0.14*	0.09	0.77	0.16 ± 0.05	0.10	0.29	0.29 ± 0.17	0.09	0.77
PO_4^{3-}-P (mg/L)	0.11 ± 0.10*	0.02	0.44	0.06 ± 0.03	0.02	0.14	0.17 ± 0.11	0.05	0.44
TOC (mg/L)	2.7 ± 0.7	1.8	5.0	2.6 ± 0.5	1.8	3.5	2.8 ± 0.8	2.2	5.0
Cl^- (mg/L)	39.88 ± 49.62	5.99	267.67	35.8 ± 63.2	5.99	267.7	44.0 ± 30.1	18.4	134.0
F^- (mg/L)	0.33 ± 0.07	0.20	0.52	0.34 ± 0.08	0.20	0.52	0.32 ± 0.06	0.27	0.44
SO_4^{2-} (mg/L)	27.17 ± 17.62	6.79	93.48	29.9 ± 22.1	6.8	93.5	24.5 ± 10.8	14.5	61.8
HCO_3^- (mg/L)	71.0 ± 30.8**	20.7	149.5	53.4 ± 17.2	20.7	85.3	88.5 ± 31.2	29.9	149.5
Na^+ (mg/L)	17.92 ± 13.66**	2.79	67.35	8.45 ± 4.87	2.79	20.29	27.4 ± 13.0	14.5	67.4
K^+ (mg/L)	4.53 ± 2.27*	1.16	11.05	3.55 ± 2.16	1.16	8.94	5.51 ± 1.93	3.71	11.05
Ca^{2+} (mg/L)	13.26 ± 7.50**	4.03	38.85	8.07 ± 3.43	4.03	16.31	18.46 ± 6.83	12.84	38.85
Mg^{2+} (mg/L)	3.24 ± 2.01**	0.52	9.83	1.97 ± 0.96	0.52	3.55	4.50 ± 1.98	1.71	9.83

N represents sample number; SD represents standard deviation; *t*-test was used to assess the seasonal differences of the hydrochemical parameters (* $p < 0.05$, ** $p < 0.01$).

0.8 °C). Average DO concentration was 5.8 ± 2.0 mg/L (range = 3.2–12.3 mg/L) implying generally oxidizing conditions in the water column. The average pH was 7.51 ± 1.05, indicating a weakly alkaline environment. The EC and TURB were 262 ± 105 μS/cm and 20.8 ± 9.9 NTU, respectively, implying moderate ionic strengths and suspended solids. The mean Chl-a during the summer wet season was 17.5 ± 24.2 μg/L, which was substantially higher than that during the winter dry season (5.3 ± 4.5 μg/L). The higher summer Chl-a concentrations were ascribed to the higher temperature and stronger solar energy promoting algal growth (Ye et al., 2022).

During the sampling period, major cation concentrations followed $Na^+ > Ca^{2+} > K^+ > Mg^{2+}$, whereas major anions followed $HCO_3^- > Cl^- > SO_4^{2-} > F^-$. Piper diagrams are frequently utilized to provide a visually geochemical characterization of water types (Ren et al., 2022). As displayed in **Fig. S2**, the main geochemical water types of the Wen-Rui Tang River were Na + K-HCO_3^- (III) and Na + Cl-SO_4^{2-} (II), the latter suggesting a possible influence from anthropogenic pollution (Xuan et al., 2020c).

TP ranged from 0.10 to 0.29 mg/L during the wet season (0.16 ± 0.05 mg/L) and from 0.09 to 0.77 mg/L during the dry season (0.29 ± 0.17 mg/L), which corresponded to a class IV water standard ($0.2 < TP \leq 0.3$ mg/L) (State Environment Protection Bureau of China, 2002). The PO_4^{3-}-P was the main form of TP and ranged from 0.02 to 0.44 mg/L. TOC concentrations ranged from 1.8 to 5.0 mg/L (2.7 ± 0.7 mg/L) with an average value of 2.6 ± 0.5 mg/L during the wet season and 2.8 ± 0.8 mg/L during the dry season.

Nitrogen pollution was elevated in the Wen-Rui Tang River network. TN concentrations ranged from 1.71 to 8.09 mg/L, with a lower average value during the wet season (2.84 ± 0.78 mg/L) than during the dry season (4.71 ± 1.22 mg/L). About 90 % of the samples exceeded the class V water quality standard of 2 mg/L (State Environment Protection Bureau of China, 2002). Average concentrations of NH_4^+-N, NO_3^--N, and NO_2^--N were 1.71 ± 1.23 mg/L (range = 0.09–5.43 mg/L), 1.09 ± 0.52 mg/L (range = 0.27–2.27 mg/L), and 0.10 ± 0.04 mg/L (range = 0.04–0.28 mg/L), respectively. On average, NH_4^+-N (45.4 %) and NO_3^--N (28.9 %) were the predominant nitrogen components of TN. PN ranged from 0.27 to 1.60 mg/L with an average of 0.75 ± 0.35 mg/L. PN was an important contributor to TN, constituting ~20 % on average. These results confirmed water quality impairment by high N concentrations in the Wen-Rui Tang River network and highlighted the need to improve the understanding of riverine N sources and transformations as a priority for developing nitrogen pollution remediation strategies.

The average concentrations for TN, NH_4^+-N, NO_3^--N, NO_2^--N, and PN during the wet and dry seasons were 2.84 mg/L versus 4.71 mg/L, 1.19 mg/L versus 2.24 mg/L, 0.92 mg/L versus 1.26 mg/L, 0.08 mg/L versus 0.12 mg/L, and 0.52 mg/L versus 0.98 mg/L, respectively (Table 1). These results implied that nitrogen contamination intensified during the winter dry season compared with the summer wet season. This phenomenon was attributed to abundant precipitation, accelerated flow rates, and augmented water column, which facilitated the dilution and dispersion of pollutant substances (Xue et al., 2024). Conversely, diminished precipitation and sluggish flow during the dry season resulted in the accumulation of N-containing pollutants in the river system. Additionally, the higher water temperatures during the wet season promoted the activity of microorganisms/algae, thereby enhancing the degradation and absorption of pollutants (Houser and Richardson, 2010). Spatial variability of TN and Cl^- in the Wen-Rui Tang River were mapped in this study. As shown in **Fig. S3**, relatively low TN and Cl^- levels were found in mainstream sites 3, 7, 9, and 12. This observation can be attributed to the diffusion processes of pollutants that were enhanced in the mainstream due to its larger volume of water compared with tributaries. Notably, TN and Cl^- concentrations at the medium level were observed at mainstream sites 1 and 2 due to these sites were in the downstream suburban areas that received pollutants not only from local villages and agricultural activities but also from upstream sources. Tributary sites 10 and 11 were located in the old urban zones of Wenzhou city characterized by high population density (**Fig. S3**). Tributary sites 5 and 13 were situated in new urban zones. These tributaries were confined and narrow, which limited the self-purification and diffusion of pollutants. Consequently, the elevated concentrations of TN in these tributary sites were attributed to the discharge of domestic sewage and the prolonged hydrological residence times in these river branches. Site 8 was located in the upstream and received the discharge of headwaters originating from mountain streams; as such, TN and Cl^- concentrations were low in this suburban site. Sites 4 and 14, located in two industrial districts, exhibited low-moderate nutrient concentrations. Currently, because of the strict ban on direct industry wastewater discharge, municipal sewage might be a

primary driver of nutrient pollution in these tributaries. Site 6, surrounded by farmland, was situated in a major grain/vegetable-producing district in the Wen-Rui Tang River watershed. Agricultural sources might be the main contributors to high TN level at site 6. Site 15 had better water quality because it was within a suburban wetland, namely, Sanyang Wetland that was stringently protected for the visitation of residents.

3.2. In-stream nitrogen transformation processes

Multiple forms of nitrogen in the water environment can transform into each other via various nitrogen biogeochemical cycling processes. The main nitrogen transformation processes in aquatic systems include ammonia volatilization, nitrification, denitrification and biological assimilation. Ammonia volatilization is a physical process that is primarily influenced by the water pH. When the pH approaches and exceeds the peak value of 9.3, NH_4^+ is readily converted to NH_3 gas and susceptible to volatilization from the water column (Kendall and McDonnell, 1998). During the sampling periods, the average pH value was 7.51 ± 1.05 (Table 1), a scenario that does not favor appreciable ammonia volatilization.

The nitrification process oxidizes NH_4^+-N to NO_3^--N as mediated by nitrifying bacteria (NH_4^+-N → NO_2^--N → NO_3^--N) (Yuan et al., 2023). High substrate concentrations (mean NH_4^+-N = 1.71 ± 1.23 mg/L) and an oxic environment (mean DO = 5.8 ± 2.0 mg/L) in the Wen-Rui Tang River provided favorable conditions for nitrification. Herein, the relationships among DO, NH_4^+-N, and NO_3^--N were assessed (**Fig. S4**). Negative relationships were found between NH_4^+-N and NO_3^--N during both the wet ($R = -0.59$, $p < 0.05$) and dry ($R = -0.61$, $p < 0.05$) seasons. By contrast, DO and NO_3^--N exhibited a positive relationship in both the wet ($R = 0.59$, $p < 0.05$) and dry ($R = 0.50$, $p = 0.058$) seasons. An expected negative relationship between DO and NH_4^+-N was also observed during the wet ($R = -0.33$, $p = 0.22$) and dry ($R = -0.71$, $p < 0.01$) seasons. These relationships were consistent with the prevalence of nitrification in the river system.

The $\delta^{18}O\text{-}NO_3^-$ values can further serve as an indicator of microbial nitrification because nitrification-derived $\delta^{18}O\text{-}NO_3^-$ values are much smaller than those of atmospheric-derived nitrate (Xuan et al., 2020a). Theoretically, one of the three oxygen atoms in NO_3^--N produced by nitrification is derived from atmospheric O_2 and the remaining two oxygen atoms are sourced from the surrounding water environment (Torres-Martínez et al., 2020). Nevertheless, this ratio has been reported to vary and is subject to change. Several recent studies demonstrated that >5/6 of all the oxygen atoms in nitrification-derived NO_3^--N can be derived from the surrounding water due to oxygen exchange (Kool et al., 2011). As depicted in Fig. 3a, majority of $\delta^{18}O\text{-}NO_3^-$ values fell within the theoretical nitrification zone, supporting the prevalence of nitrification in the Wen-Rui Tang River network.

Nitrifying bacteria further consume DO and preferentially utilize the lighter $^{14}N\text{-}NH_4^+$ isotope resulting in the enrichment of the remaining $^{15}N\text{-}NH_4^+$ as concentrations of NO_3^--N increase and NH_4^+-N decrease. However, the expected correlations between $\delta^{15}N\text{-}NH_4^+$ and NO_3^--N/NH_4^+-N concentrations in the water samples were not evident (Fig. 3bc). This apparent discrepancy may result from large N pollution inputs and the co-occurrence of multiple nitrogen transformation processes altering the overall concentrations and isotopic composition of NO_3^--N and NH_4^+-

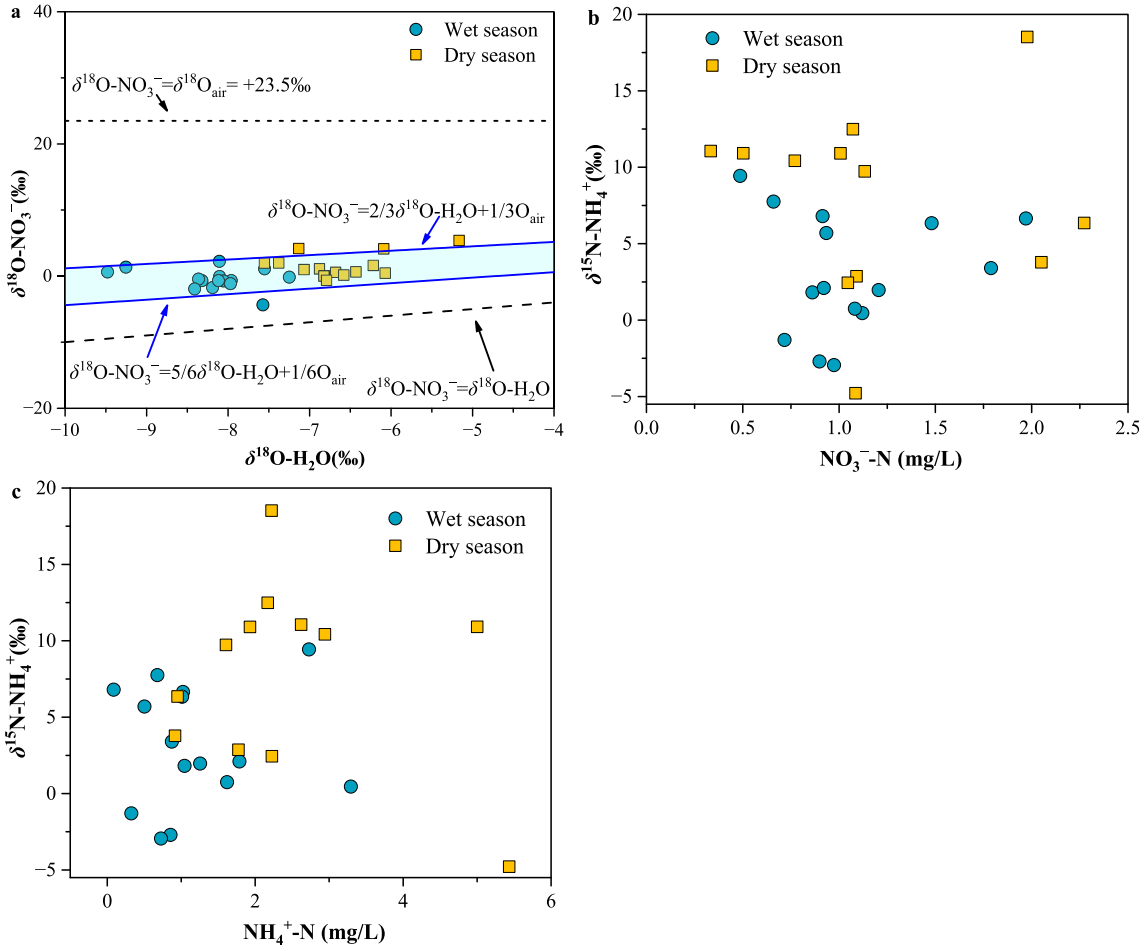

Fig. 3. Relationships between (a) $\delta^{18}O\text{-}NO_3^-$ and $\delta^{18}O\text{-}H_2O$, (b) $\delta^{15}N\text{-}NH_4^+$ and NO_3^--N, and (c) $\delta^{15}N\text{-}NH_4^+$ and NH_4^+-N in the Wen-Rui Tang River network during the wet and dry seasons. The solid blue area in panel-a is the theoretical nitrification zone.

N. Despite the lack of statistical significance among some aforementioned relationships, the overall isotopic and hydrochemical information supported that nitrification was a predominant N-cycling process.

Denitrification (NO_3^--N → NO_2^--N → NO → N_2O → N_2) consumes NO_3^--N, leading to a simultaneous increase in δ^{15}N-NO_3^- and δ^{18}O-NO_3^- with a ratio ranging from 1.3: 1 to 2.1: 1 (Zhao et al., 2023). The plot of δ^{15}N-NO_3^- versus δ^{18}O-NO_3^- did not exhibit a distinct denitrification pattern (Fig. 4a). Moreover, there was not a significant negative relationship between δ^{15}N-NO_3^- and NO_3^--N concentrations (Fig. 4b). Generally, denitrification occurs under anaerobic condition with DO concentration < 2 mg/L (Archana et al., 2018). During the study periods, DO concentrations were sufficiently high (mean = 5.8 mg/L) to hinder the denitrification process within the water column, although some denitrification could occur in the anaerobic riverine sediments. All these lines of evidence implied that in-stream denitrification was not a prevalent nitrogen transformation process in the Wen-Rui Tang River network.

Heterogeneous nitrogen sources and competing transformation processes could mask the denitrification signals. As a result, although the isotopic patterns and aerobic conditions did not support widespread in-stream denitrification as a dominant process, some denitrification could occur in localized hotspots within the river network, such as in hyporheic and riparian zones (Cey et al., 1999; Hale et al., 2014; Deng et al., 2020). In the future, additional targeted studies are warrantied to clarify the prevalence of the denitrification process in the Wen-Rui Tang River via microbial DNA techniques.

N_2O stable isotopes can be used to determine the production process of N_2O (i.e., bacterial denitrification, nitrifier denitrification, and nitrification) based on their distinct $\delta^{15}N^{bulk}$/SP/δ^{18}O-N_2O values (Toyoda et al., 2011; Ibraim et al., 2019). For example, the reported SP-N_2O values for bacterial denitrification, nitrifier denitrification, and nitrification are −0.8 ± 5.8 ‰, −0.5 ± 1.9 ‰, and 33.5 ± 1.2 ‰ respectively; δ^{18}O-N_2O values for bacterial denitrification, nitrifier denitrification, and nitrification range from 17.4 to 21.4 ‰, 19.8 to 26.5 ‰, and 36.5 to 55.2 ‰, respectively; and $\delta^{15}N^{bulk}$ values for bacterial denitrification/nitrifier denitrification and nitrification range from 0 to 37 ‰, and from 30.9 to 68 ‰, respectively (Koba et al., 2009; Rohe et al., 2014; Lewicka-Szczebak et al., 2016; Denk et al., 2017). The SP-N_2O and δ^{18}O-N_2O values for the Wen-Rui Tang River samples varied from 41.7 to 62.8 ‰ and from 17.3 to 36.8 ‰, respectively (Fig. 4c). The scatter of SP-N_2O versus δ^{18}O-N_2O values were generally close to the range for nitrification, which confirmed that nitrification was a prevalent N-cycling process in the watershed. Moreover, some points were located in the region between the nitrification and denitrification zones. This outcome suggested denitrification could generate some dissolved N_2O within denitrification hotspots.

For the Wen-Rui Tang River, high concentrations of NH_4^+-N (1.71 ± 1.23 mg/L) and NO_3^--N (1.09 ± 0.52 mg/L) provided an abundant source of nitrogen for phytoplankton assimilation. The concentrations of Chl-a were moderately high during the summer wet season (17.5 ± 24.2 μg/L; Table 1). During the N assimilation process, microbes, such as algae and phytoplankton, uptake NH_4^+-N and NO_3^--N with a preference for the lighter isotope (^{14}N). This situation leads to an increase of δ^{15}N-NH_4^+/NO_3^- and a 1:1 enrichment between δ^{15}N-NO_3^- and δ^{18}O-NO_3^-

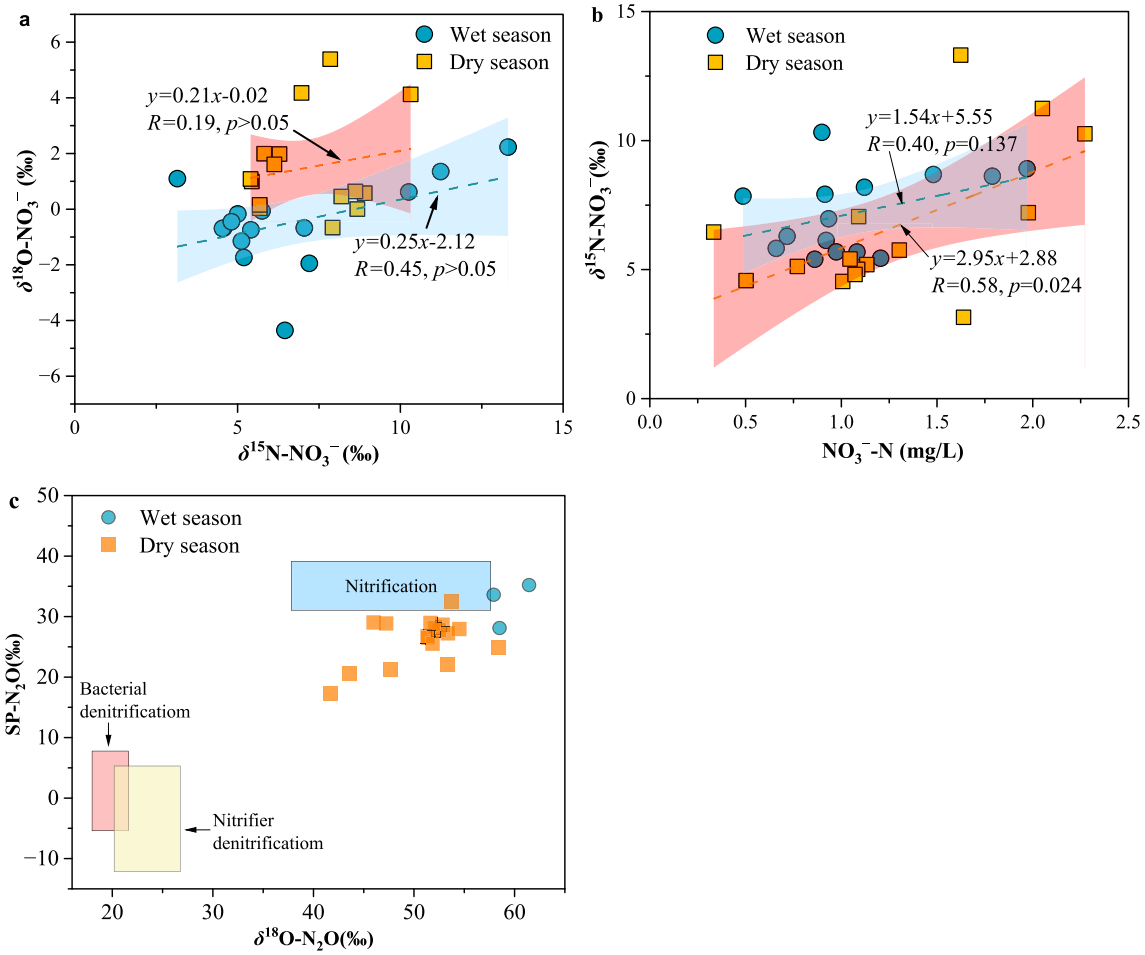

Fig. 4. Relationships between (a) δ^{15}N-NO_3^- and δ^{18}O-NO_3^-, (b) δ^{15}N-NO_3^- and NO_3^--N, and (c) δ^{18}O-N_2O and site preference(SP) of N_2O in the Wen-Rui Tang River network during the wet and dry seasons. Light bands indicate 95 % confidence of the relationship.

(Granger et al., 2004; Fry, 2006). The δ^{15}N-PN values ranged from −3.64 to 7.98 ‰ with an average value of 0.37 ‰; these values were lower than those for δ^{15}N-NH_4^+/NO_3^- (Fig. 5). Weak negative correlations were observed between δ^{15}N-PN and δ^{15}N-NH_4^+ during the wet ($R = -0.54$, $p = 0.073$) and dry ($R = -0.48$, $p = 0.07$) seasons, whereas no negative correlation was found between δ^{15}N-PN and δ^{15}N-NO_3^-. Importantly, the PN fraction originated from both living/dead aquatic primary production and exogenous organic matter from the terrestrial environment. Hence, the PN fraction did not solely represent the primary production within the riverine environment.

These isotopic patterns and Chl-a contents indicated a potential role for biological assimilation in affecting nitrogen isotope composition in the Wen-Rui Tang River, with the wet season having higher assimilation compared with the dry season. The greater assimilation in the summer wet period was favored by the higher temperature and light conditions that promoted phytoplankton growth. In addition, NH_4^+-N was preferentially consumed by phytoplankton versus NO_3^--N (Glibert et al., 2016), which supported a stronger negative relationship between δ^{15}N-PN and δ^{15}N-NH_4^+ versus that between δ^{15}N-PN and δ^{15}N-NO_3^-. With these considerations, we posited that biological assimilation of N was not a dominant process regulating the inorganic nitrogen forms and isotope compositions in the Wen-Rui Tang River.

Based on the aforementioned interpretations of the predominant processes governing nitrogen transformations, we concluded that microbial nitrification was the dominant process with lesser contributions from biological assimilation and denitrification during the study periods. The occurrence of in-stream ammonia volatilization was deemed negligible due to the near-neutral pH values of most surface water samples.

3.3. Identification of nitrogen sources

Stable isotopes have been widely used to investigate the contributions of various pollution sources to riverine NO_3^--N (Fadhullah et al., 2020; Ren et al., 2022). The δ^{15}N-NO_3^- values in the Wen-Rui Tang River ranged from 3.15 to 13.31 ‰ (6.61 ± 2.74 ‰) during the wet season and from 5.40 to 10.32 ‰ (7.19 ± 1.50 ‰) during the dry season (Fig. 6a). δ^{18}O-NO_3^- values ranged from −4.36 to 2.23 ‰ (−0.49 ± 1.51 ‰) during the wet season and from −0.66 to 5.39 ‰ (1.50 ± 1.71 ‰) during the dry season (Fig. 6a). Among the 30 surface water samples, 8 samples were located within the domain of a municipal sewage source, 8 samples were in a mixed domain of soil nitrogen and municipal sewage, and 13 samples were in a mixed domain of nitrogen fertilizer, soil nitrogen and municipal sewage. Interpreting Fig. 6a, the main NO_3^--N source in the Wen-Rui Tang River network was municipal sewage, followed by soil nitrogen and nitrogen fertilizer. A greater number of samples collected during the wet season were located within nitrogen fertilizer and soil nitrogen source ranges because the greater rainfall during this period causing increased leaching of nitrogen fertilizer and soil nitrogen.

The δ^{15}N-NH_4^+ values varied from 2.44 to 18.52 ‰ (9.04 ± 4.59 ‰) during the wet season and from 4.67 to 13.06 ‰ (9.53 ± 2.29 ‰) during the dry season (Fig. 6b). Most samples were within the range of sewage, indicating that domestic sewage was the primary source of NH_4^+-N during the study period. The average values of δ^{15}N-PN were 1.07 ± 2.57 ‰ (range: −3.64 to 7.98 ‰) for the wet season and − 0.33 ± 1.77 ‰ (range: −2.20 to 3.56 ‰) for the dry season. As depicted in Fig. 6c, the δ^{15}N-PN values encompassed a range below that of sewage, indicating that suspended PN likely originated from soil nitrogen rather than domestic sewage. Notably, these qualitative identification results contained a high degree of uncertainty because the isotopic compositions of riverine NH_4^+-N, NO_3^--N, and suspended PN can be altered by N-cycling processes, including nitrification, denitrification and biological assimilation.

Chloride can be an effective indicator of human/animal excreta and domestic sewage due to its incorporation into animal diets and its conservative characteristic in natural waters (Nyilitya et al., 2021; Chen et al., 2023b). Generally, low Cl^- concentrations and high NO_3^--N/Cl^- ratios indicate pollution from agricultural sources, whereas high Cl^- concentrations and low NO_3^--N/Cl^- ratios are characteristic of manure/domestic sewage (Jin et al., 2019; Chen et al., 2023a). As shown in **Fig. S5a**, almost all samples were located in the area comprising a dominance of manure/sewage, providing support that the NO_3^--N in the Wen-Rui Tang River was strongly influenced by pollution from manure/sewage sources. Moreover, the increased number of samples from the area close to agricultural pollution sources during the wet season revealed a greater contribution from agricultural sources during the summer wet season. Significant positive correlations were observed between Cl^- and TN during the wet ($R = 0.80$, $p < 0.01$) and dry ($R = 0.81$, $p < 0.01$; with outlier removed) seasons (**Fig. S5b**). These positive relationships further suggested that the TN loads were strongly influenced by municipal sewage discharge, which was fully consistent with the aforementioned isotopic analyses.

3.4. Contributions of pollution sources to riverine nitrogen

Although the multi-isotope method can qualitatively identify the main nitrogen sources, quantitative information on nitrogen sources is necessary to assist decision makers in developing nitrogen pollution remediation strategies. In this study, a SIAR model-TN source apportionment method was employed to calculate the proportional contributions of nitrogen sources to riverine TN pollution. In this study, we assumed that nitrogen pollution in the Wen-Rui Tang River was derived

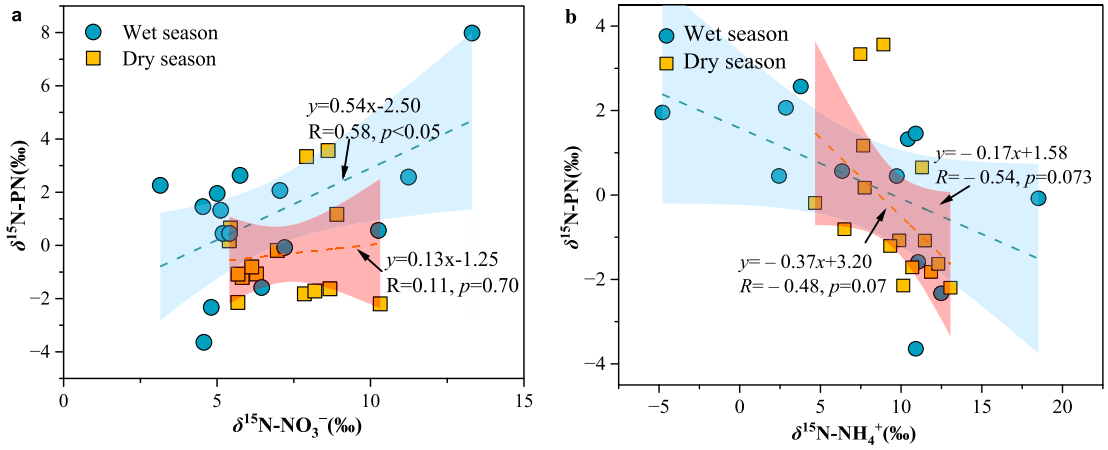

Fig. 5. Relationships between (a) δ^{15}N-PN and δ^{15}N-NO_3^- and (b) δ^{15}N-PN and δ^{15}N-NH_4^+ in the Wen-Rui Tang River network during the wet and dry seasons. Light bands indicate 95 % confidence of the relationship.

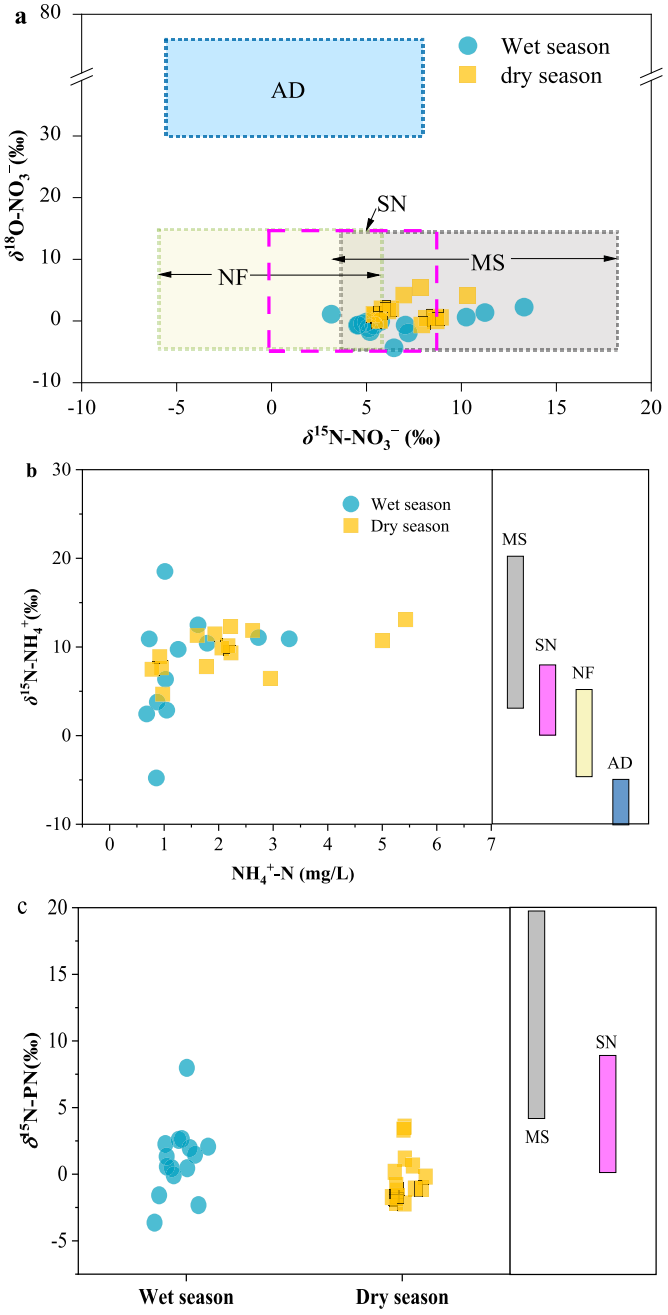

Fig. 6. (a) Cross-plot of riverine δ^{18}O-NO_3^- versus δ^{15}N-NO_3^- values, (b) ammonia nitrogen isotopic signatures (δ^{15}N-NH_4^+), and (c) suspended particulate nitrogen isotopic signatures (δ^{15}N-PN) in the Wen-Rui Tang River network during the wet and dry seasons.AD: atmospheric deposition, NF: nitrogen fertilizer, SN: soil nitrogen, MS: municipal sewage.

from external pollution sources including atmospheric deposition, nitrogen fertilizer, soil nitrogen, and municipal sewage. The isotopic compositions of potential pollution sources were determined using samples collected from the Wen-Rui Tang River watershed (**Table S1**). Since there was no significant effect of denitrification on isotopic signatures of NO_3^--N, the SIAR model was executed with a fractionation coefficient of 0 during the modeling process. Herein, the DON and NO_2^--N sources were not considered, and the sources contributing to these two nitrogen constituents were ascribed to other pollution sources (Fig. 7). The reasons were as follows: (1) DON and NO_2^--N were minor nitrogen forms contributing ~5 % of the overall TN content in the Wen-Rui Tang River network, and (2) currently, it is difficult to apportion the DON sources owing to the complexity of determining the $^{15}N/^{14}N$ ratios for DON.

The relative contributions of nitrogen pollution sources to the TN loads of the Wen-Rui Tang River are shown in Fig. 7. Municipal sewage was the largest source contributing 40.6 % during the wet season and 59.1 % during the dry season. Soil nitrogen was also a major source adding 39.5 % and 30.4 % for the wet and dry seasons, respectively. Lower contributions were provided by nitrogen fertilizer (9.7 % and 4.1 % for the wet and dry seasons, respectively) and atmospheric deposition (2.8 % and 1.0 % for the wet and dry seasons, respectively). In the Wen-Rui Tang River watershed, the large amount of precipitation during the wet season could accelerate the leaching of nitrogen fertilizer and soil nitrogen to nearby stream channels. Intensive agricultural practices, such as nitrogen fertilizer application, irrigation, and tillage during the wet season, might be another reason for the elevated nitrogen fertilizer and soil nitrogen contributions. In contrast, reduced precipitation level and low-intensity agricultural practices in the dry season led to a lower proportion of riverine nitrogen from nitrogen fertilizer and soil nitrogen sources, and a correspondingly higher proportion from the municipal sewage source. Our results are consistent with previous findings, which showed higher contributions from municipal sewage and smaller contributions from nitrogen fertilizer and soil nitrogen in the dry season (Ji et al., 2017; Liu et al., 2018; Li et al., 2019). As shown in **Fig. S6**, uncertainty analysis results showed that uncertainties associated with potential pollution sources within the Wen-Rui Tang River watershed were different. The UI_{90} values for each nitrogen source followed the order soil nitrogen (0.505 and 0.333) > municipal sewage (0.466 and 0.297) > nitrogen fertilizer (0.247 and 0.105) > atmospheric deposition (0.083 and 0.0286) during the wet and dry seasons, respectively. This result implied that the contribution of atmospheric deposition was quite stable while the uncertainty of soil nitrogen contribution was strongest. Municipal sewage and nitrogen fertilizer source contributions exhibited a moderate degree of uncertainty.

3.5. Implications

This study was conducted in a typical coastal-plain river network, which is widely distributed in coastal regions around the world. These regions boast a well-developed economy, high levels of urbanization, and a high population density, contributing to elevated levels of nitrogen inputs into waterways. Multiple stable isotopes including δ^{15}N/δ^{18}O-NO_3^-, δ^{15}N-NH_4^+, δ^{15}N-PN, δ^{18}O-H_2O, and $\delta^{15}N^{bulk}/\delta^{18}$O/SP-$N_2O$ were investigated to capture a comprehensive understanding of nitrogen cycling processes and sources. Relying only on δ^{15}N/δ^{18}O-NO_3^- failed to present a holistic perspective regarding nitrogen pollution owing to the multiple forms of nitrogen input to the river network. Additionally, phytoplankton exhibited a preference for utilizing NH_4^+-N instead of NO_3^--N as their primary nitrogen source; thus, δ^{15}N/δ^{18}O-NO_3^- did not identify the biological assimilation process when NH_4^+-N was the dominant form of phytoplankton uptake (Xuan et al., 2020b).

This study highlighted the importance of using multiple stable isotopes to obtain more information and further insights into nitrogen cycling processes and sources. For instance, δ^{15}N-NH_4^+ can be utilized for the identification of NH_4^+-N sources and assimilation/nitrification processes; δ^{15}N-PN can be employed to identify PN sources and assimilation; and $\delta^{15}N^{bulk}/\delta^{18}$O/SP-$N_2O$ can identify nitrification/denitrification processes, while δ^{18}O-H_2O was useful in identifying nitrification (Li et al., 2022; Liang et al., 2022; Zhang et al., 2022). Furthermore, isotopic fractionation during N-cycling processes (e.g., nitrification and assimilation) will simultaneously change the isotopic composition of products (e.g., NO_3^--N for nitrification and PN for assimilation) and substrates (e.g., NH_4^+-N for nitrification and assimilation). We can reduce the influence of isotopic fractionation based on analysis of multiple isotopes, thereby providing more accurate proportional contributions of pollution sources to the TN loads (not limited to the NO_3^--N) via the SIAR model. The findings derived from this study

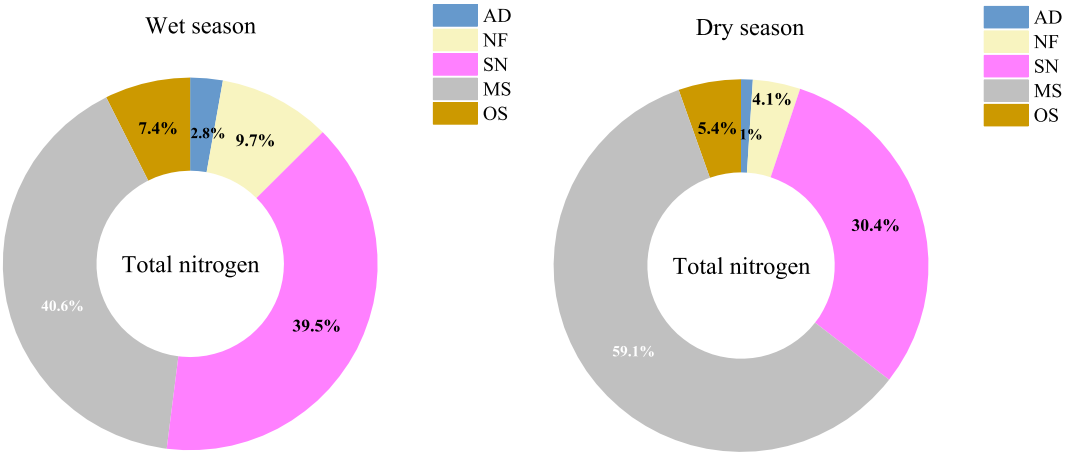

Fig. 7. Contributions of potential pollution sources to total nitrogen in the Wen-Rui Tang River network during the wet and dry seasons. AD: atmospheric deposition, NF: nitrogen fertilizer, SN: soil nitrogen, MS: municipal sewage, OS: other sources.

will enable local government agencies to design more targeted nitrogen management strategies.

The results of the multiple isotope methods confirmed the predominance of municipal sewage-sourced nitrogen pollution in the Wen-Rui Tang River. With continuing urbanization and increasing population, municipal sewage contributions to the Wen-Rui Tang River are expected to increase. Consequently, sewage effluent requires greater overall collection and treatment, such as construction of new wastewater treatment plants offering secondary and tertiary treatment options. Furthermore, expanding the sewage pipeline network, diverting storm runoff and wastewater, and upgrade/repair of the aging pipeline network are necessary to prevent untreated sewage from entering the river network. Meanwhile, it is recommended to implement best management practices including riparian plantings, buffer strips, and constructed/restored wetlands to reduce soil nitrogen and nitrogen fertilizer leaching during the wet season.

4. Conclusions

In our study, multiple hydrochemical parameters and stable isotopic values were investigated in a coastal-plain river system in Eastern China to elucidate transformations and sources of riverine nitrogen. Over 90 % of the water samples exceeded the class V standard of 2 mg/L for TN in surface waters of China. NH_4^+-N, NO_3^--N, and PN coexisted in the surface waters comprising 45.4 %, 28.9 %, and 19.9 % of TN, respectively. Multiple hydrochemical and isotopic evidence identified microbial nitrification as the prevailing nitrogen cycling process. Biological assimilation and denitrification were considered minor processes, and ammonia volatilization was deemed negligible. A SIAR model-TN source apportionment method was developed to distinguish TN sources to guide pollution remediation. SIAR modeling of TN source apportionment calculated the following source contributions: Wet season; municipal sewage (40.6 %) ≈ soil nitrogen (39.5 %) > nitrogen fertilizer (9.7 %) > atmospheric deposition (2.8 %) versus Dry season; municipal sewage (59.1 %) > soil nitrogen (30.4 %) > nitrogen fertilizer (4.1 %) > atmospheric deposition (1.0 %). The novel aspect of this study was the identification of N-cycling process and TN pollution sources in plain river networks by combining multi-component nitrogen isotopic compositions with a SIAR model, which provided substantially more detail and reliability than previous studies that utilized only $\delta^{15}N/\delta^{18}O\text{-}NO_3^-$ information. In the future, the development of new technologies to include DON source isotopes could further improve the overall TN source apportionment results, especially in waters containing high levels of DON. Moreover, the introduction of microbial DNA techniques in conjunction with the multi-isotope analysis would confirm the importance of individual nitrogen cycling processes.

Ethical approval

Not applicable.

Consent to participate

Not applicable.

Consent to publish

Not applicable.

Funding

This work was funded by the National Natural Science Foundation of China (Grant Nos. 42307104 and 51979197), Natural Science Foundation of Zhejiang Province (Grant No. LTGS23D030002), Science and Technology Project of Wenzhou Science and Technology Bureau (Grant No. S20220014), Science Research Funding of Wenzhou Medical University (Grant No. KYYW202220), Science and Technology Innovation Program for College Students in Zhejiang Province (Grant No. 2023R413080), and National College Students Innovation and Entrepreneurship Training Program (Grant No. 202210343011). The authors are grateful to Lielin Shu for conducting water quality investigation.

CRediT authorship contribution statement

Wenli Chen: Writing – original draft, Investigation, Funding acquisition, Formal analysis. **Xiaohan Zhang:** Investigation. **Nianting Wu:** Investigation. **Can Yuan:** Investigation. **Yinli Liu:** Investigation, Funding acquisition. **Yue Yang:** Supervision, Resources, Investigation, Conceptualization. **Zheng Chen:** Supervision. **Randy A. Dahlgren:** Writing – review & editing, Writing – original draft, Supervision, Methodology, Conceptualization. **Minghua Zhang:** Writing – review & editing, Supervision, Funding acquisition. **Xiaoliang Ji:** Writing – review & editing, Writing – original draft, Supervision, Methodology, Investigation, Funding acquisition, Formal analysis, Conceptualization.

Declaration of competing interest

The authors declare no competing financial interests.

Data availability

Data will be made available on request.

Appendix A. Supplementary data

Supplementary data to this article can be found online at https://doi.org/10.1016/j.scitotenv.2024.171671.

References

Archana, A., Thibodeau, B., Geeraert, N., Xu, M.N., Kao, S.J., Baker, D.M., 2018. Nitrogen sources and cycling revealed by dual isotopes of nitrate in a complex urbanized environment. Water Res. 142, 459–470. https://doi.org/10.1016/j.watres.2018.06.004.

Cao, M., Hu, A., Gad, M., Adyari, B., Qin, D., Zhang, L., Sun, Q., Yu, C.P., 2022. Domestic wastewater causes nitrate pollution in an agricultural watershed. China. Sci. Total Environ. 823, 153680 https://doi.org/10.1016/j.scitotenv.2022.153680.

Cey, E.E., Rudolph, D.L., Aravena, R., Parkin, G., 1999. Role of the riparian zone in controlling the distribution and fate of agricultural nitrogen near a small stream in southern Ontario. J. Contam. Hydrol. 37, 45–67. https://doi.org/10.1016/S0169-7722(98)00162-4.

Chen, R., Hu, Q., Shen, W., Guo, J., Yang, L., Yuan, Q., Lu, X., Wang, L., 2023a. Identification of nitrate sources of groundwater and rivers in complex urban environments based on isotopic and hydro-chemical evidence. Sci. Total Environ. 871, 162026 https://doi.org/10.1016/j.scitotenv.2023.162026.

Chen, X., Zheng, L., Zhu, M., Jiang, C., Dong, X., Chen, Y., 2023b. Quantitative identification of nitrate and sulfate sources of a multiple land-use area impacted by mine drainage. J. Environ. Manag. 325, 116551 https://doi.org/10.1016/j.jenvman.2022.116551.

Deng, D., Pan, Y., Liu, G., Liu, W., Ma, L., 2020. Seeking the hotspots of nitrogen removal: a comparison of sediment denitrification rate and denitrifier abundance among wetland types with different hydrological conditions. Sci. Total Environ. 737, 140253 https://doi.org/10.1016/j.scitotenv.2020.140253.

Denk, T.R.A., Mohn, J., Decock, C., Lewicka-Szczebak, D., Harris, E., Butterbach-Bahl, K., Kiese, R., Wolf, B., 2017. The nitrogen cycle: a review of isotope effects and isotope modeling approaches. Soil Biol. Biochem. 105, 121–137. https://doi.org/10.1016/j.soilbio.2016.11.015.

Dong, J., Zhao, X., Liu, C., Huang, Z., Qadeer, A., Zhu, Y., Wang, H., Zheng, B., 2022. Multi-isotope tracing nitrate dynamics and sources during thermal stratification in a deep reservoir. Chemosphere 307, 135816. https://doi.org/10.1016/j.chemosphere.2022.135816.

Fackrell, J.K., Kraus, T.E.C., Young, M.B., Kendall, C., Peek, S., 2022. Stable isotopes provide insight into sources and cycling of N compounds in the Sacramento-san Joaquin Delta, California, USA. Sci. Total Environ. 816, 151592 https://doi.org/10.1016/j.scitotenv.2021.151592.

Fadhullah, W., Yaccob, N.S., Syakir, M.I., Muhammad, S.A., Yue, F.-J., Li, S.-L., 2020. Nitrate sources and processes in the surface water of a tropical reservoir by stable isotopes and mixing model. Sci. Total Environ. 700, 134517 https://doi.org/10.1016/j.scitotenv.2019.134517.

Fry, B., 2006. Stable Isotope Ecology. Springer, USA, New York.

Gibrilla, A., Fianko, J.R., Ganyaglo, S., Adomako, D., Anornu, G., Zakaria, N., 2020. Nitrate contamination and source apportionment in surface and groundwater in Ghana using dual isotopes (^{15}N and ^{18}O-NO_3) and a Bayesian isotope mixing model. J. Contam. Hydrol. 233, 103658 https://doi.org/10.1016/j.jconhyd.2020.103658.

Glibert, P.M., Wilkerson, F.P., Dugdale, R.C., Raven, J.A., Dupont, C.L., Leavitt, P.R., Parker, A.E., Burkholder, J.M., Kana, T.M., 2016. Pluses and minuses of ammonium and nitrate uptake and assimilation by phytoplankton and implications for productivity and community composition, with emphasis on nitrogen-enriched conditions. Limnol. Oceanogr. 61 (1), 165–197. https://doi.org/10.1002/lno.10203.

Granger, J., Sigman, D.M., Needoba, J.A., Harrison, P.J., 2004. Coupled nitrogen and oxygen isotope fractionation of nitrate during assimilation by cultures of marine phytoplankton. Limnol. Oceanogr. 49, 1763–1773. https://doi.org/10.4319/lo.2004.49.5.1763.

Guo, W., Zhang, D., Zhang, W., Li, S., Pan, K., Jiang, H., Zhang, Q., 2023. Anthropogenic impacts on the nitrate pollution in an urban river: insights from a combination of natural-abundance and paired isotopes. J. Environ. Manag. 333, 117458 https://doi.org/10.1016/j.jenvman.2023.117458.

Guo, Z., Yan, C., Wang, Z., Xu, F., Yang, F., 2020. Quantitative identification of nitrate sources in a coastal peri-urban watershed using hydrogeochemical indicators and dual isotopes together with the statistical approaches. Chemosphere 243, 125364. https://doi.org/10.1016/j.chemosphere.2019.125364.

Hale, R.L., Turnbull, L., Earl, S., Grimm, N., Riha, K., Michalski, G., Lohse, K.A., Childers, D., 2014. Sources and transport of nitrogen in arid urban watersheds. Environ. Sci. Technol. 48, 6211–6219. https://doi.org/10.1021/es501039t.

Houser, J.N., Richardson, W.B., 2010. Nitrogen and phosphorus in the upper Mississippi River: transport, processing, and effects on the river ecosystem. Hydrobiologia 640, 71–88. https://doi.org/10.1007/s10750-009-0067-4.

Ibraim, E., Wolf, B., Harris, E., Gasche, R., Wei, J., Yu, L., Kiese, R., Eggleston, S., Butterbach-Bahl, K., Zeeman, M., Tuzson, B., Emmenegger, L., Six, J., Henne, S., Mohn, J., 2019. Attribution of N_2O sources in a grassland soil with laser spectroscopy based isotopocule analysis. Biogeosciences 16, 3247–3266. https://doi.org/10.5194/bg-16-3247-2019.

Ji, X., Xie, R., Hao, Y., Lu, J., 2017. Quantitative identification of nitrate pollution sources and uncertainty analysis based on dual isotope approach in an agricultural watershed. Environ. Pollut. 229, 586–594. https://doi.org/10.1016/j.envpol.2017.06.100.

Ji, X., Shu, L., Chen, W., Chen, Z., Shang, X., Yang, Y., Dahlgren, R.A., Zhang, M., 2022a. Nitrate pollution source apportionment, uncertainty and sensitivity analysis across a rural-urban river network based on $\delta^{15}N/\delta^{18}O$-$NO_3^-$ isotopes and SIAR modeling. J. Hazard. Mater. 438, 129480 https://doi.org/10.1016/j.jhazmat.2022.129480.

Ji, X., Shu, L., Li, J., Zhao, C., Chen, W., Chen, Z., Shang, X., Dahlgren, R.A., Yang, Y., Zhang, M., 2022b. Tracing nitrate sources and transformations using $\Delta^{17}O$, $\delta^{15}N$, and $\delta^{18}O$-NO_3^- in a coastal plain river network of eastern China. J. Hydrol. 610, 127829 https://doi.org/10.1016/j.jhydrol.2022.127829.

Jin, Z., Cen, J., Hu, Y., Li, L., Shi, Y., Fu, G., Li, F., 2019. Quantifying nitrate sources in a large reservoir for drinking water by using stable isotopes and a Bayesian isotope mixing model. Environ. Sci. Pollut. Res. 26, 20364–20376. https://doi.org/10.1007/s11356-019-05296-7.

Kendall, C., McDonnell, J.J., 1998. Isotope Tracers in Catchment Hydrology. Elsevier Science.

Kim, S.H., Lee, D.H., Kim, M.S., Rhee, H.P., Hur, J., Shin, K.H., 2023. Systematic tracing of nitrate sources in a complex river catchment: an integrated approach using stable isotopes and hydrological models. Water Res. 235, 119755 https://doi.org/10.1016/j.watres.2023.119755.

Koba, K., Osaka, K., Tobari, Y., Toyoda, S., Ohte, N., Katsuyama, M., Suzuki, N., Itoh, M., Yamagishi, H., Kawasaki, M., Kim, S.J., Yoshida, N., Nakajima, T., 2009. Biogeochemistry of nitrous oxide in groundwater in a forested ecosystem elucidated by nitrous oxide isotopomer measurements. Geochim. Cosmochim. Acta 73, 3115–3133. https://doi.org/10.1016/j.gca.2009.03.022.

Kohl, D.H., Shearer, G.B., Commoner, B., 1971. Fertilizer nitrogen: contribution to nitrate in surface water in a corn belt watershed. Science 174, 1331–1334. https://doi.org/10.1126/science.174.4016.1331.

Kool, D.M., Wrage, N., Oenema, O., Van Kessel, C., Van Groenigen, J.W., 2011. Oxygen exchange with water alters the oxygen isotopic signature of nitrate in soil ecosystems. Soil Biol. Biochem. 43, 1180–1185. https://doi.org/10.1016/j.soilbio.2011.02.006.

Lewicka-Szczebak, D., Dyckmans, J., Kaiser, J., Marca, A., Augustin, J., Well, R., 2016. Oxygen isotope fractionation during N_2O production by soil denitrification. Biogeosciences 13, 1129–1144. https://doi.org/10.5194/bg-13-1129-2016.

Li, C., Li, S.L., Yue, F.J., Liu, J., Zhong, J., Yan, Z.F., Zhang, R.C., Wang, Z.J., Xu, S., 2019. Identification of sources and transformations of nitrate in the Xijiang River using nitrate isotopes and Bayesian model. Sci. Total Environ. 646, 801–810. https://doi.org/10.1016/j.scitotenv.2018.07.345.

Li, S., Wang, S., Ji, G., 2022. Influences of carbon sources on N_2O production during denitrification in freshwaters: activity, isotopes and functional microbes. Water Res. 226, 119315 https://doi.org/10.1016/j.watres.2022.119315.

Li, X., Tang, C., Cao, Y., Li, X., 2021. Isotope and isotopomer ratios of dissolved N_2O as indicators of nitrogen apportionment and transformation in shallow groundwater in Dongguan, southern China. J. Hydrol. 600, 126514 https://doi.org/10.1016/j.jhydrol.2021.126514.

Lian, X., Zhu, G., Yang, W., Zhu, M., Xu, H., 2020. Effect of heavy rainfall on nitrogen and phosphorus concentrations in rivers at river-net plain. Environ. Sci. 41, 4970–4980. (in Chinese). 10.13227/j.hjkx.202003183.

Liang, X., Wang, B., Gao, D., Han, P., Zheng, Y., Yin, G., Dong, H., Tang, Y., Hou, L., 2022. Nitrification regulates the spatiotemporal variability of N_2O emissions in a eutrophic lake. Environ. Sci. Technol. 56, 17430–17442. https://doi.org/10.1021/acs.est.2c03992.

Liu, J., Shen, Z., Yan, T., Yang, Y., 2018. Source identification and impact of landscape pattern on riverine nitrogen pollution in a typical urbanized watershed, Beijing. China. Sci. Total Environ. 628-629, 1296–1307. https://doi.org/10.1016/j.scitotenv.2018.02.161.

Liu, J., Yan, T., Shen, Z., 2021. Sources, transformations of suspended particulate organic matter and their linkage with landscape patterns in the urbanized Beiyun river watershed of Beijing. China. Sci. Total Environ. 791, 148309 https://doi.org/10.1016/j.scitotenv.2021.148309.

Lu, H., Chen, X., Zhao, H., Zou, Y., Qian, X., 2021. Characteristics of nitrogen and phosphorus status of surface water in rural medium and small rivers in a plain river network region of North Jiangsu Province. Water Resour. Prot. 28 (5), 1–6 (in Chinese).

Nyilitya, B., Mureithi, S., Bauters, M., Boeckx, P., 2021. Nitrate source apportionment in the complex Nyando tropical river basin in Kenya. J. Hydrol. 594, 125926 https://doi.org/10.1016/j.jhydrol.2020.125926.

Parnell, A.C., Inger, R., Bearhop, S., Jackson, A.L., 2010. Source partitioning using stable isotopes: coping with too much variation. PLoS One 5 (3), e9672. https://doi.org/10.1371/journal.pone.0009672.

Ren, K., Pan, X., Yuan, D., Zeng, J., Liang, J., Peng, C., 2022. Nitrate sources and nitrogen dynamics in a karst aquifer with mixed nitrogen inputs (Southwest China): revealed by multiple stable isotopic and hydro-chemical proxies. Water Res. 210, 118000 https://doi.org/10.1016/j.watres.2021.118000.

Rohe, L., Anderson, T.H., Braker, G., Flessa, H., Giesemann, A., Lewicka-Szczebak, D., Wrage-Mönnig, N., Well, R., 2014. Dual isotope and isotopomer signatures of nitrous oxide from fungal denitrification-a pure culture study. Rapid Commun. Mass Sp. 28, 1893–1903. https://doi.org/10.1002/rcm.6975.

Ryu, H., Kim, S., Baek, U., Kim, D., Lee, H., Chung, E., Kim, M., Kim, K., Lee, J., 2021. Identifying nitrogen sources in intensive livestock farming watershed with swine excreta treatment facility using dual ammonium ($\delta^{15}N_{NH4}$) and nitrate ($\delta^{15}N_{NO3}$) nitrogen isotope ratios axes. Sci. Total Environ. 779, 146480 https://doi.org/10.1016/j.scitotenv.2021.146480.

Shang, X., Huang, H., Mei, K., Xia, F., Chen, Z., Yang, Y., Dahlgren, R.A., Zhang, M., Ji, X., 2020. Riverine nitrate source apportionment using dual stable isotopes in a drinking water source watershed of Southeast China. Sci. Total Environ. 724, 137975 https://doi.org/10.1016/j.scitotenv.2020.137975.

Soto, D.X., Koehler, G., Wassenaar, L.I., Hobson, K.A., 2019. Spatio-temporal variation of nitrate sources to Lake Winnipeg using N and O isotope ($\delta^{15}N$, $\delta^{18}O$) analyses. Sci. Total Environ. 647, 486–493. https://doi.org/10.1016/j.scitotenv.2018.07.346.

State Environment Protection Bureau of China, 2002. Environmental Quality Standards for Surface Water (GB3838–2002). China Environmental Science Press, Beijing (in Chinese).

Tian, S., Gaye, B., Tang, J., Luo, Y., Li, W., Lahajnar, N., Dähnke, K., Sanders, T., Xiong, T., Zhai, W., Emeis, K.C., 2022. A nitrate budget of the Bohai Sea based on an isotope mass balance model. Biogeosciences 19, 2397–2415. https://doi.org/10.5194/bg-19-2397-2022.

Torres-Martínez, J.A., Mora, A., Knappett, P.S.K., Ornelas-Soto, N., Mahlknecht, J., 2020. Tracking nitrate and sulfate sources in groundwater of an urbanized valley using a multi-tracer approach combined with a Bayesian isotope mixing model. Water Res. 182, 115962 https://doi.org/10.1016/j.watres.2020.115962.

Torres-Martínez, J.A., Mora, A., Mahlknecht, J., Daesle, L.W., Cervantes-Aviles, P.A., Ledesma-Ruiz, R., 2021a. Estimation of nitrate pollution sources and transformations in groundwater of an intensive livestock-agricultural area (Comarca Lagunera), combining major ions, stable isotopes and MixSIAR model. Environ. Pollut. 269, 115445 https://doi.org/10.1016/j.envpol.2020.115445.

Torres-Martínez, J.A., Mora, A., Mahlknecht, J., Kaown, D., Barceló, D., 2021b. Determining nitrate and sulfate pollution sources and transformations in a coastal aquifer impacted by seawater intrusion-a multi-isotopic approach combined with self-organizing maps and a Bayesian mixing model. J. Hazard. Mater. 417, 126103 https://doi.org/10.1016/j.jhazmat.2021.126103.

Toyoda, S., Yano, M., Nishimura, S., Akiyama, H., Hayakawa, A., Koba, K., Sudo, S., Yagi, K., Makabe, A., Tobari, Y., Ogawa, N.O., Ohkouchi, N., Yamada, K., Yoshida, N., 2011. Characterization and production and consumption processes of N_2O emitted from temperate agricultural soils determined via isotopomer ratio analysis. Glob. Biogeochem. Cycles 25, GB2008. https://doi.org/10.1029/2009GB003769.

Xuan, Y., Tang, C., Cao, Y., 2020a. Mechanisms of nitrate accumulation in highly urbanized rivers: evidence from multi-isotopes in the Pearl River Delta. China. J. Hydrol. 587, 124924 https://doi.org/10.1016/j.jhydrol.2020.124924.

Xuan, Y., Tang, C., Liu, G., Cao, Y., 2020b. Carbon and nitrogen isotopic records of effects of urbanization and hydrology on particulate and sedimentary organic matter in the highly urbanized Pearl River Delta. China. J. Hydrol. 591, 125565 https://doi.org/10.1016/J.JHYDROL.2020.125565.

Xuan, Y.X., Cao, Y.J., Tang, C.Y., Li, M., 2020c. Changes in dissolved inorganic carbon in river water due to urbanization revealed by hydrochemistry and carbon isotope in the Pearl River Delta. China.Environ. Sci. Pollut. Res. 27, 24542–24557. https://doi.org/10.1007/s11356-020-08454-4.

Xue, D., Botte, J., De Baets, B., Accoe, F., Nestler, A., Taylor, P., Van Cleemput, O., Berglund, M., Boeckx, P., 2009. Present limitations and future prospects of stable isotope methods for nitrate source identification in surface- and groundwater. Water Res. 43, 1159–1170. https://doi.org/10.1016/j.watres.2008.12.048.

Xue, J., Yuan, C., Ji, X., Zhang, M., 2024. Predictive modeling of nitrogen and phosphorus concentrations in rivers using a machine learning framework: a case study in an urban-rural transitional area in Wenzhou China. Sci. Total Environ. 910, 168521 https://doi.org/10.1016/j.scitotenv.2023.168521.

Ye, F., Jia, G., Wei, G., Guo, W., 2022. A multi-stable isotopic constraint on water column oxygen sinks in the Pearl River estuary. South China. Mar. Environ. Res. 178, 105643 https://doi.org/10.1016/j.marenvres.2022.105643.

Ye, H., Tang, C., Cao, Y., 2021. Sources and transformation mechanisms of inorganic nitrogen: evidence from multi-isotopes in a rural-urban river area. Sci. Total Environ. 794, 148615 https://doi.org/10.1016/j.scitotenv.2021.148615.

Yi, Q., Chen, Q., Hu, L., Shi, W., 2017. Tracking nitrogen sources, transformation, and transport at a basin scale with complex plain river networks. Environ. Sci. Technol. 51, 5396–5403. https://doi.org/10.1021/acs.est.6b06278.

Yuan, B., Guo, M., Zhou, X., Li, M., Xie, S., 2023. Defining the sources and the fate of nitrate by using dual isotopes and a Bayesian isotope mixing model: water–nitrate management in cascade dams of Lancang River. Sci. Total Environ. 886, 163995 https://doi.org/10.1016/j.scitotenv.2023.163995.

Zhang, A., Lei, K., Lang, Q., Li, Y., 2022. Identification of nitrogen sources and cycling along freshwater river to estuarine water continuum using multiple stable isotopes. Sci. Total Environ. 851, 158136 https://doi.org/10.1016/j.scitotenv.2022.158136.

Zhang, H., Xu, Y., Cheng, S., Li, Q., Yu, H., 2020. Application of the dual-isotope approach and Bayesian isotope mixing model to identify nitrate in groundwater of a multiple land-use area in Chengdu plain. China. Sci. Total Environ. 717, 137134 https://doi.org/10.1016/j.scitotenv.2020.137134.

Zhao, G., Sun, T., Wang, D., Chen, S., Ding, Y., Li, Y., Shi, G., Sun, H., Wu, S., Li, Y., Wu, C., Li, Y., Yu, Z., Chen, Z., 2023. Treated wastewater and weak removal mechanisms enhance nitrate pollution in metropolitan rivers. Environ. Res. 231, 116182 https://doi.org/10.1016/j.envres.2023.116182.